Structural Basis for a Ca^{2+}-Sensing Function of the Metabotropic Glutamate Receptors

Yoshihiro Kubo,* Tomoyuki Miyashita, Yoshimichi Murata

The metabotropic glutamate receptors (mGluRs) are widely distributed in the brain and play important roles in synaptic plasticity. Here it is shown that some types of mGluRs are activated not only by glutamate but also by extracellular Ca^{2+} (Ca^{2+}_o). A single amino acid residue was found to determine the sensitivity of mGluRs to Ca^{2+}_o. One of the receptors, mGluR1α, but not its point mutant with reduced sensitivity to Ca^{2+}_o, caused morphological changes when transfected into mammalian cells. Thus, the sensing of Ca^{2+}_o by mGluRs may be important in cells under physiological condition.

The mGluRs are a family of heterotrimeric guanosine triphosphate–binding protein (G protein)–coupled receptors (*1*, *2*) that exist in various regions of the brain (*3*) and are known to play an important role in synaptic plasticity (*4*). Because of the structural similarity of mGluRs and the Ca^{2+}_o sensor of the parathyroid (*2*, *5*, *6*), we tested whether mGluRs function as Ca^{2+} sensors. We previously showed that a mGluR1 homolog isolated from the salmon brain can be activated not only by glutamate but also by Ca^{2+}_o (*7*). Here we investigated whether rat mGluR1α and mGluR5 (which couple to G_q) and mGluR2 and mGluR3 (which couple to G_i) are activated by Ca^{2+}_o.

The responses of mGluRs 1α and 5 to Ca^{2+}_o were examined by monitoring the increase in Ca^{2+}-activated Cl^- (Ca^{2+}-Cl^-) current in a *Xenopus laevis* oocyte expression system (*8*). The oocytes were bathed in Ca^{2+}-free saline solution, and then the Ca^{2+}_o concentration ($[Ca^{2+}]_o$) was increased while depolarizing pulses were applied. Oocytes expressing either mGluR1α or mGluR5 responded to 2 mM Ca^{2+}, whereas noninjected oocytes did not (Fig. 1A). The response increased steeply in the physiological range of $[Ca^{2+}]_o$ (Fig. 1A), similarly to the response of the Ca^{2+} receptor (CaR) (*5*, *6*, *9*). When $[Ca^{2+}]_o$ was raised, we also detected increases of the inositol trisphosphate (IP_3) concentration in oocytes expressing mGluR1α (*7*) and of the intracellular concentration of Ca^{2+} ($[Ca^{2+}]_i$) in transfected CHO cells by Fluo-3 imaging (*10*). Because the CaR is activated not only by Ca^{2+} but also by various polyvalent cations (*5*), we examined the effects of polyvalent cations on mGluRs 1α and 5. Both were activated by polyvalent cations (Fig. 1B). Similar to the CaR (*5*), trivalent cations such as Gd^{3+} (Fig. 1B) were more effective than Ca^{2+} in activating mGluRs 1α and 5. Divalent cations other than Ca^{2+} (Fig. 1B) were less effective. Thus, mGluR1α and mGluR5 sense Ca^{2+}_o and polyvalent cations as does the CaR.

The responses of the G_i-coupled mGluRs 2 and 3 were monitored by an increase in inward current of the coexpressed G protein–coupled, inwardly rectifying K^+ channel, GIRK1/2 (*11*), in *Xenopus* oocytes (*8*). mGluR3 was activated by Ca^{2+} as well as glutamate, whereas mGluR2 showed no response to 5 mM Ca^{2+}_o (Fig. 1C). The response of mGluR3 to Ca^{2+}_o

Y. Kubo and T. Miyashita, Department of Neurophysiology, Tokyo Metropolitan Institute for Neuroscience, Musashidai 2-6, Fuchu, Tokyo 183-8526, Japan.
Y. Murata, Department of Neurophysiology, Tokyo Metropolitan Institute for Neuroscience, Musashidai 2-6, Fuchu, Tokyo 183-8526, Japan, and Department of Medical Physiology, Meiji College of Pharmacy, Nozawa 1-35-23, Setagaya, Tokyo 154-003, Japan.

*To whom correspondence should be addressed. E-mail: ykubo@tmin.ac.jp

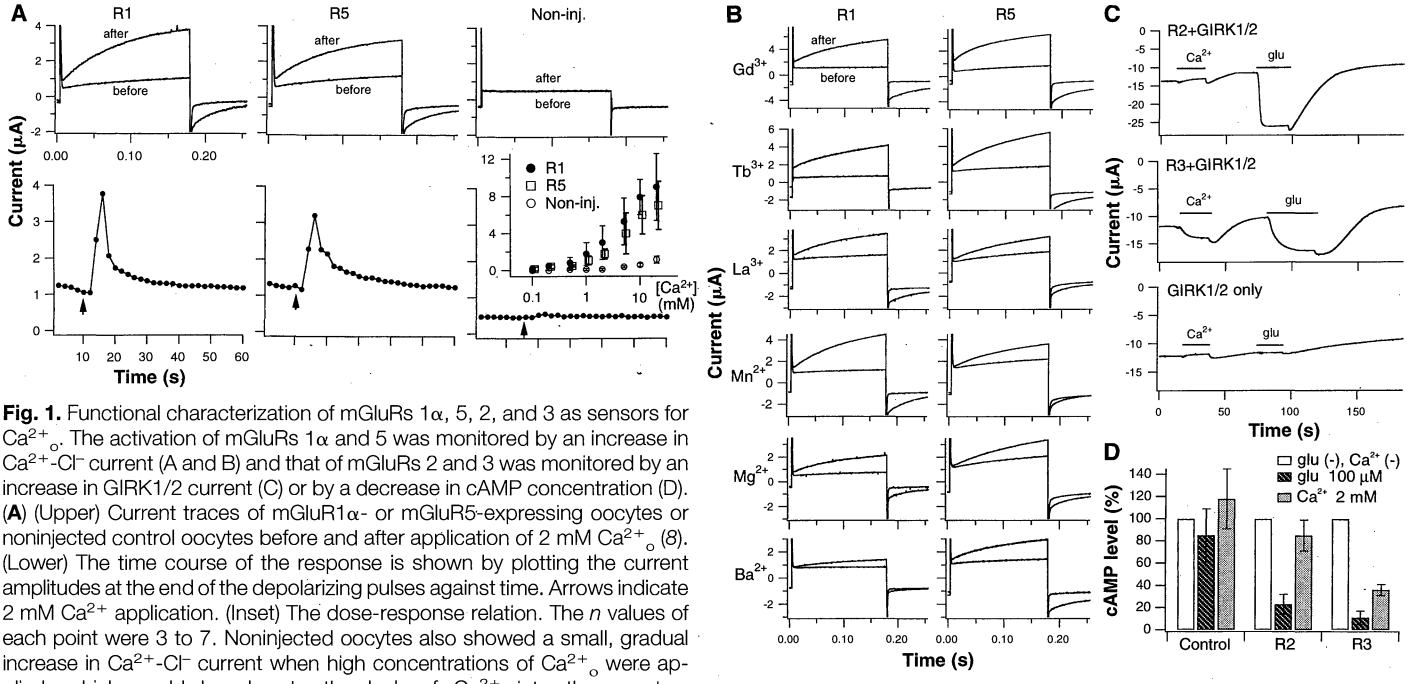

Fig. 1. Functional characterization of mGluRs 1α, 5, 2, and 3 as sensors for Ca^{2+}_o. The activation of mGluRs 1α and 5 was monitored by an increase in Ca^{2+}-Cl^- current (A and B) and that of mGluRs 2 and 3 was monitored by an increase in GIRK1/2 current (C) or by a decrease in cAMP concentration (D). (**A**) (Upper) Current traces of mGluR1α- or mGluR5-expressing oocytes or noninjected control oocytes before and after application of 2 mM Ca^{2+}_o (*8*). (Lower) The time course of the response is shown by plotting the current amplitudes at the end of the depolarizing pulses against time. Arrows indicate 2 mM Ca^{2+} application. (Inset) The dose-response relation. The *n* values of each point were 3 to 7. Noninjected oocytes also showed a small, gradual increase in Ca^{2+}-Cl^- current when high concentrations of Ca^{2+}_o were applied, which could be due to the leak of Ca^{2+} into the oocytes. (**B**) Current traces before and after application of 1 mM Gd^{3+}, Tb^{3+}, or La^{3+} or 10 mM Mn^{2+}, Mg^{2+}, or Ba^{2+} to oocytes expressing mGluR1α or mGluR5. (**C**) Current traces recorded at –120 mV from oocytes expressing mGluR2 and GIRK1/2, mGluR3 and GIRK1/2, or GIRK1/2 alone. Either 40 μM glutamate (glu) or 5 mM Ca^{2+}_o was applied at the times indicated by the bars. (**D**) Effect of glutamate or Ca^{2+}_o to the cAMP concentration in CHO cell lines stably transfected with vector alone, mGluR2 cDNA, or mGluR3 cDNA (*18*). The cAMP concentrations were normalized by the concentration in the absence of glutamate or Ca^{2+}_o. The error bars indicate standard deviation (n = 3).

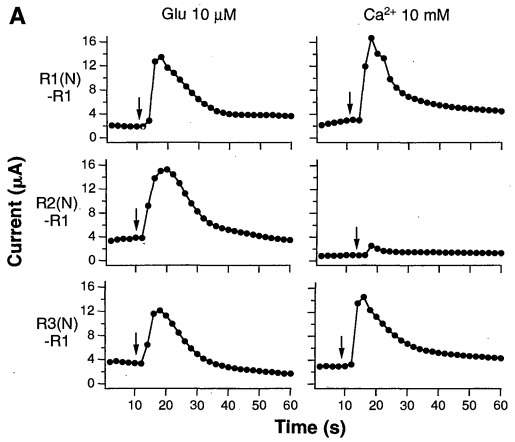

Fig. 2. Comparison of the responses of R1(N)-R1, R2(N)-R1, and R3(N)-R1 chimeras to glutamate or $Ca^{2+}{}_o$. (**A**) Examples of responses of R1(N)-R1, R2(N)-R1, and R3(N)-R1 to 10 μM glutamate (Glu) (left) or to 10 mM $Ca^{2+}{}_o$ (right). (**B**) Comparison of the dose-response relations of R1(N)-R1, R2(N)-R1, and R3(N)-R1 to glutamate (left) or $Ca^{2+}{}_o$(right). The *n* values of each point are 3 to 7. The EC_{50} values of the fittings were as follows: glutamate (R1, 4.6 μM; R2(N)-R1, 6.4 μM; R3(N)-R1, 7.2 μM) and $Ca^{2+}{}_o$ (R1, 4.7 mM; R2(N)-R1, 36.0 mM; R3(N)-R1, 2.2 mM). Three sets of data in each plot were obtained from the same batch of oocytes.

varied between batches of oocytes. A response was detected in three out of nine batches, and in the three positive batches, the responses were observed in three out of five, two out of five, and two out of three oocytes. These results suggest that the link between $Ca^{2+}{}_o$ and activation of GIRK1/2 current by mGluR3 requires additional endogenous conditions. Even in the positive cells, an accurate dose-response analysis was not possible because the amplitude of the responses could not be determined accurately as a result of the decrease in the basal current level after the agonist was removed. The possible link of $Ca^{2+}{}_o$ stimulation with G_i was also confirmed as a decrease in the adenosine 3′,5′-monophosphate (cAMP) concentration by $Ca^{2+}{}_o$ in mGluR3-transfected CHO cells but not in mGluR2-transfected cells (Fig. 1D).

To make a quantitative comparison of the $Ca^{2+}{}_o$-sensing properties of mGluRs 1α, 2, and 3, we assayed the activity of the same effector. Chimeric molecules were constructed in which the entire NH_2-terminal extracellular domain of mGluR2 or mGluR3 was substituted for that of mGluR1α [R2(N)-R1 and R3(N)-R1, respectively] (*12*). R2(N)-R1 and R3(N)-R1 chimeras were expected to link to G_q proteins and activate Ca^{2+}-Cl^- currents similar to mGluR1α. The sensitivity of these molecules to glutamate or $Ca^{2+}{}_o$ was compared (Fig. 2) (*8*). The median effective concentration (EC_{50}) values of the dose-response relation to glutamate did not differ significantly from each other. In contrast, the EC_{50} value of R2(N)-R1 to $Ca^{2+}{}_o$ (36.0 mM) was significantly higher than those of mGluR1α (4.7 mM) and R3(N)-R1 (2.2 mM) (Fig. 2B). Thus, mGluR1α and mGluR3 appear to be more sensitive to $Ca^{2+}{}_o$ than is mGluR2, and the structural basis of the $Ca^{2+}{}_o$ sensitivity would be predicted to lie in the NH_2-terminal extracellular domain.

To identify the structural determinant of $Ca^{2+}{}_o$ sensitivity within the NH_2-terminal extracellular region, we tested whether the $Ca^{2+}{}_o$-sensing site overlapped with the glutamate-binding site (*8*). After exposure to the saturating dose of glutamate (or $Ca^{2+}{}_o$), mGluR1α still responded to $Ca^{2+}{}_o$ (or glutamate) (Fig. 3A). Thus, there was no strong cross-desensitization, suggesting that $Ca^{2+}{}_o$ and glutamate are not recognized in an identical manner by mGluR1α. The re-

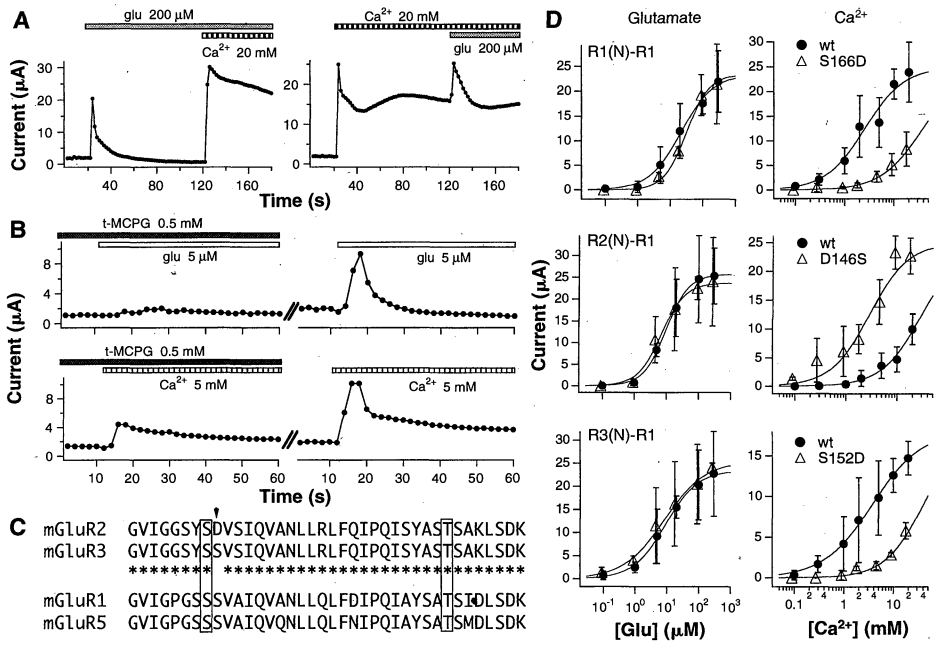

Fig. 3. Identification of the site responsible for the $Ca^{2+}{}_o$-sensing function of mGluRs. (**A**) Effect of a saturating dose of glutamate (or $Ca^{2+}{}_o$) to the response of mGluR1α to $Ca^{2+}{}_o$ (or glutamate). (**B**) Effect of t-MCPG on glutamate- or $Ca^{2+}{}_o$-induced responses in oocytes expressing mGluR1α. The two traces on the left and right are from the same oocyte. A concentration of 0.5 mM t-MCPG, which almost completely blocked the response to 5 μM glutamate, partially blocked the response to an equivalent dose (5 mM) of $Ca^{2+}{}_o$. (**C**) Alignments of the deduced amino acid sequences of mGluRs 2, 3, 1α, and 5 in the region adjacent to the glutamate-binding sites. The glutamate-binding sites, S165(R1) and T188(R1), are boxed, and the site that determines the sensitivity to $Ca^{2+}{}_o$ (S166 in R1) is shown by the arrow (*19*). (**D**) Comparison of the dose-response relations of the wild type (wt) (filled circles) and the point mutants (open triangles) of R1(N)-R1, R2(N)-R1, and R3(N)-R1. Sites shown by the arrow in (C) were mutated to D in R1 and R3, and to S in R2. The *n* value of each point was 3 to 7. The EC_{50} values of the fittings were as follows: glutamate (R1-wt, 22 μM; R1-mut, 32 μM; R2-wt, 9.6 μM; R2-mut, 6.9 μM; R3-wt, 9.1 μM; R3-mut, 8.4 μM) and $Ca^{2+}{}_o$ (R1-wt, 2.5 mM; R1-mut, 39 mM; R2-wt, 30 mM; R2-mut, 2.9 mM; R3-wt, 3.7 mM; R3-mut, 41 mM). Two sets of data in each plot are from the same batch of oocytes. The larger EC_{50} values for the glutamate response of wild-type mGluR1α and the mutant compared with the value in Fig. 2B was due to the difference in the batch of oocytes.

sponse of mGluR1α to 5 mM Ca^{2+}_o was partially blocked by 0.5 mM t-MCPG (*S*-α-methyl-4-carboxyphenylglycine), which inhibited the response to glutamate of the equivalent dose (5 μM) almost completely (Fig. 3B). Thus, the Ca^{2+}_o-interacting site appears to be not identical to but to overlap with the glutamate-binding site.

Structural and mutagenesis analyses previously revealed that the glutamate-binding sites of mGluR1α are located at Ser^{165} and Thr^{188} (*13*). The amino acid sequences of mGluRs 1α, 2, 3, and 5 in the region adjacent to these sites were compared (Fig. 3C). Although mGluRs 2 and 3 exhibit high identity in this region, the residue next to the glutamate-binding site differs. The mGluRs 1α, 3, and 5 have a serine (S) at this position whereas mGluR2 has an aspartate (D). Thus, we hypothesized that this site determines the Ca^{2+}_o sensitivity of mGluRs and examined the properties of the point mutants R1(N)-R1 (S166D), R2(N)-R1 (D146S), and R(3)-R1 (S152D) (*8*, *12*). These mutations did not alter sensitivity to glutamate but did change the sensitivity to Ca^{2+}_o (Fig. 3D). S166D of R1(N)-R1 and S152D of R3(N)-R1 showed much lower sensitivity to Ca^{2+}_o than the wild type, and D146S of R2(N)-R1 had a high sensitivity to Ca^{2+}_o (Fig. 3D). Thus, this site (S166 of mGluR1α) was critical for the determination of the sensitivity to Ca^{2+}_o.

The above results were obtained by monitoring responses when $[Ca^{2+}]_o$ was abruptly raised from 0 mM. It is important to know if the continuous stimulation by physiological concentrations of Ca^{2+}_o through mGluR1α causes some intracellular events (that is, if the Ca^{2+}_o-sensing function of mGluR1α plays a role under physiological conditions). We transfected CHO cells with wild-type mGluR1α or with the S166D mutant transiently (*14*) and compared the cell morphology (Fig. 4A) and the alignment of actin filaments (Fig. 4B) (*15*). To analyze the cell morphology quantitatively, we classified the cells by a morphology index (the ratio of the long axis length to the short axis length). Control CHO cells mostly exhibited a square-shaped morphology, but the cells transfected with wild-type mGluR1α, identified by cotransfected green fluorescent protein (GFP), changed to a spindle or a bar shape (Fig. 4, A and C). The actin filaments of the transfected cells identified by antibody to mGluR1α (anti-mGluR1) were aligned in parallel (Fig. 4, B and C). In contrast, the morphological change of CHO cells transfected with the S166D mutant was much less (Fig. 4). When $[Ca^{2+}]$ in the culture medium was raised from 2 to 5 mM, the morphological change of the cells transfected with wild-type mGluR1α was more prominent, but control cells did not respond at all (*10*). Thus, the continuous stimulation of mGluR1α by 2 mM Ca^{2+} in the medium caused the parallel alignments of the actin filaments and the morphological change of the transfected CHO cells, probably by means of an increase in second messenger activity. Indeed, the basal IP_3 concentration in oocytes expressing mGluR1α in the frog saline solution was higher than in noninjected oocytes (*7*), and the cAMP concentration in CHO cells expressing mGluR1α was elevated not only by glutamate (*16*) but also by Ca^{2+}_o (0 mM Ca^{2+}_o, 100%; 2 mM, 148%; 10 mM, 180%), whereas cAMP in control cells was not elevated (0 mM Ca^{2+}_o,100%; 2 mM, 77%, 10 mM, 96%).

What is the significance of the Ca^{2+}-sensing function of mGluRs in the brain? As demonstrated above, it is possible that constant stimulation by Ca^{2+}_o would cause an increase in the basal activity of the second messenger system such as IP_3, protein kinase C, or cAMP in neurons expressing mGluR1α. This increase might play a role, for example, in the maintenance phase of long-term potentiation. Another possibility is that the dynamic fluctuation of $[Ca^{2+}]_o$ in the synaptic cleft might stimulate mGluR1α effectively. The local $[Ca^{2+}]_o$ in the narrow synaptic cleft is not constant but could fluctuate in the range between 0.8 and 1.5 mM (*17*). An increase of Ca^{2+}_o from 0.5 mM (or 1 mM) to 1.5

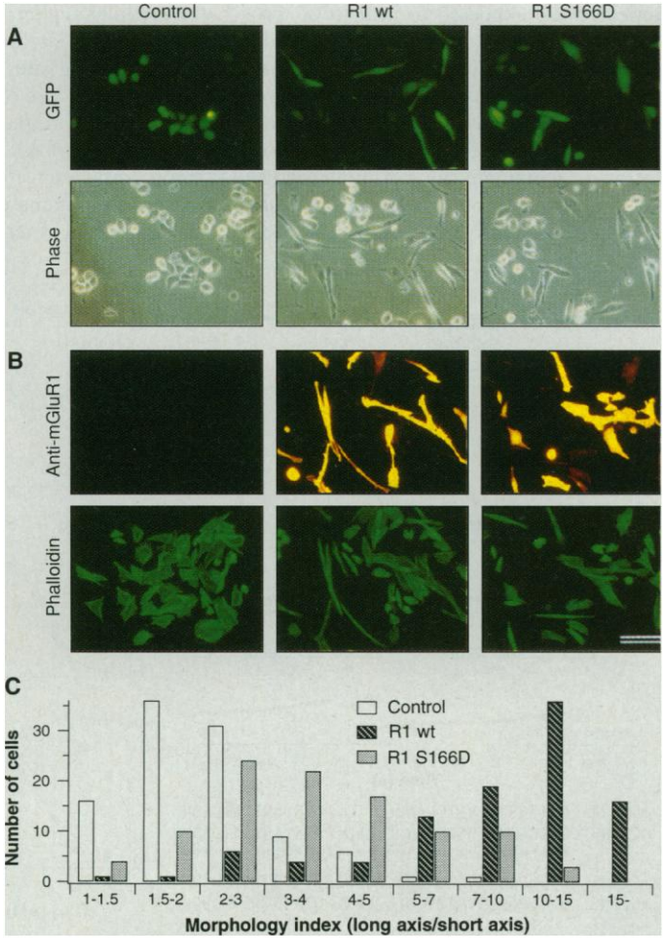

Fig. 4. Comparison of the morphology of control CHO cells and CHO cells transfected with wild-type mGluR1α (R1 wt) or with the S166D mutant (R1 S166D). (**A**) Observations of the living CHO cells transfected with pEGFP alone (left), wild type and pEGFP (middle), or S166D and pEGFP (right). The transfected cells were identified by the fluorescence of GFP (upper panels), and the morphology of the identified cells was observed with a phase-contrast microscope (lower panels). The scale bar in (B) indicates 100 μm for all photographs in (A) and (B). (**B**) Morphology of the actin filaments of CHO cells transfected with vector alone (left), wild-type mGluR1α (middle), or S166D (right). The cells transfected with mGluR1α were identified by staining with anti-mGluR1 (upper row, middle and right panels). The actin filaments were visualized by staining with FITC-phalloidin (lower panels). (**C**) Quantitative analysis of the cell morphology of the three groups in (B). The cells were classified into nine classes by the morphology index, and the number of cells of each class are shown.

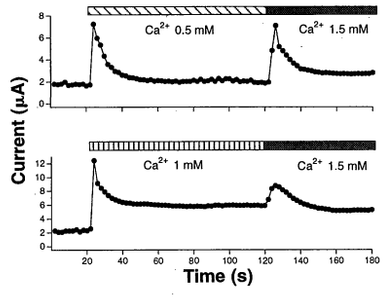

Fig. 5. Effect of $[Ca^{2+}_o]$ fluctuation on mGluR1α expressed in *Xenopus* oocytes. The $[Ca^{2+}_o]$ was changed in the range known to occur physiologically at the synaptic cleft (*17*).

mM caused responses in oocytes expressing mGluR1α (Fig. 5). It is possible that the activation of mGluR1α would be triggered by the fluctuation of local $[Ca^{2+}]_o$ in the synaptic cleft.

Thus, mGluRs 1α, 5, and 3 but not mGluR2 are activated by $Ca^{2+}{}_o$ at physiological concentrations, and a single amino acid residue determines the sensitivity to $Ca^{2+}{}_o$. Also, the $Ca^{2+}{}_o$-sensing function of mGluR1α can play a role in generating morphological changes in transfected cells.

REFERENCES AND NOTES

1. H. Sugiyama, I. Ito, C. Hirono, *Nature* **325**, 531 (1987); M. Masu, Y. Tanabe, K. Tsuchida, R. Shigemoto, S. Nakanishi, *ibid.* **349**, 760 (1991); Y. Tanabe, M. Masu, T. Ishii, R. Shigemoto, S. Nakanishi, *Neuron* **8**, 169 (1992); T. Abe *et al.*, *J. Biol. Chem.* **267**, 13361 (1992); Y. Nakajima *et al.*, *ibid.* **268**, 11868 (1993); N. Okamoto *et al.*, *ibid.* **269**, 1231 (1994).
2. R. M. Duvoisin, C. Zhang, K. Ramonell, *J. Neurosci.* **15**, 3075 (1995).
3. S. Nakanishi, *Science* **258**, 597 (1992); R. Shigemoto *et al.*, *J. Neurosci.* **17**, 7503 (1997).
4. R. Shigemoto *et al.*, *Neuron* **12**, 1245 (1994); A. Aiba *et al.*, *Cell* **79**, 365 (1994); A. Aiba *et al.*, *ibid.*, p. 377; M. Kano *et al.*, *Neuron* **18**, 71 (1997).
5. E. M. Brown *et al.*, *Nature* **366**, 575 (1993).
6. J. E. Garrett *et al.*, *J. Biol. Chem.* **270**, 12919 (1995).
7. K. Kubokawa *et al.*, *FEBS Lett.* **392**, 71 (1996).
8. Complementary RNA for injection into oocytes was prepared with an in vitro transcription kit (Stratagene), and the yield was estimated by loading cRNA onto an agarose gel. Noninjected oocytes were used as a negative control. Preparation of *Xenopus* oocytes and the two-electrode voltage clamp experiments were carried out as described (*7*). The standard saline solution for culturing oocytes contained 88 mM NaCl, 1 mM KCl, 0.3 mM $Ca(NO_3)_2$, 0.41 mM $CaCl_2$, 0.8 mM $MgSO_4$, 2.4 mM $NaHCO_3$, and 15 mM Hepes (pH 7.6). In the experiments of Fig. 1, A and B, Fig. 2, A and B, Fig. 3, A, B, and D, and Fig. 5, the Ca^{2+}-free saline (0 mM Ca^{2+}, 0.3 mM Mg^{2+}), which contained 88 mM NaCl, 1 mM KCl, 2.4 mM $NaHCO_3$, 0.3 mM $MgCl_2$, and 15 mM Hepes (pH 7.6), was used to reduce the basal level of the Ca^{2+}-Cl^- current. The concentration of Mg^{2+} was held at 0.3 mM to suppress the leak current level. The Ca^{2+}-Cl^- current was monitored by applying depolarizing pulses of 175 ms to 60 mV every 2 s from the holding potential of −80 mV. While the oocytes were being given the repeated depolarizing pulses, one-fifth volume of 5× concentrated stock solutions of polyvalent cations or glutamate was applied gently to the bath, so that the flow was not directed at the oocyte, and then mixed immediately and thoroughly with a pipette. In the experiments of Fig. 1C, a high-K^+ solution containing 90 mM KCl, 0.3 mM $MgCl_2$, and 10 mM Hepes (pH 7.5) was used.
9. D. Riccardi *et al.*, *Proc. Natl. Acad. Sci. U.S.A.* **92**, 131 (1995); M. Ruat *et al.*, *ibid.*, p. 3161.
10. Y. Kubo, T. Miyashita, Y. Murata, unpublished observation.
11. Y. Kubo, E. Reuveny, P. A. Slesinger, Y. N. Jan, L. Y. Jan, *Nature* **364**, 802 (1993); N. Dascal *et al.*, *Proc. Natl. Acad. Sci. U.S.A.* **90**, 10235 (1993); F. Lesage *et al.*, *J. Biol. Chem.* **270**, 28660 (1995).
12. Chimeric molecules were prepared as follows. A unique Eco RV site was introduced at the very end of the NH_2-terminal cytoplasmic region of mGluRs 1α, 2, and 3 by mutagenesis with Sculptor kit (Amersham). These mutations did not cause amino acid substitution in mGluR1α and caused one mutation in mGluR2 (A566I, in which Ala at position 566 is mutated to Ile) and in mGluR3 (A575I). These amino acid substitutions did not affect the responses. The introduced Eco RV sites were then used to prepare chimeric molecules R2(N)-R1 and R3(N)-R1. The point mutants in Fig. 3D were also prepared with Sculptor kit (Amersham), and the sequences of the primer regions were determined by a DNA sequencer (ABI 377). To avoid unexpected mutations, we confirmed that two independent clones of the same mutation showed identical properties.
13. P. J. O'Hara *et al.*, *Neuron* **11**, 41 (1993).
14. To minimize the glutamate concentration in the medium, we cultured CHO cells in glutamine-free Dulbecco's minimum essential medium (DMEM) (2 mM Ca^{2+}) and 10% dialyzed fetal bovine serum (Gibco). Instead of glutamine, GlutaMAX-1(Gibco) at a reduced concentration of 2 mM was added to the medium just before use and the medium was changed twice a day. Wild-type mGluR1α and the S166D mutant were subcloned into $pCXN_2$ expression vector [H. Niwa, K. Yamamura, J. Miyazaki, *Gene* **108**, 193 (1991)] and then transiently transfected into CHO cells with Lipofectamine Plus (Gibco). Forty-eight hours later, the living cells were observed or fixed with 4% paraformaldehyde and 0.2% picrinic acid for immunohistochemistry analysis. For observation of living cells, pEGFP (Clonetech) was cotransfected to identify transfected cells. For the experiment in Fig. 1D, a CHO cell line stably expressing mGluR3 was established by G418 (Gibco) selection.
15. The transfected cells were identified by staining with polyclonal antibody to mGluR1 (Chemicon) and Cy3-labeled secondary antibody (Jackson ImmunoResearch Labs, West Grove, PA). The morphology of the actin filaments was visualized by staining with fluorescein isothiocyanate (FITC)–labeled phalloidin.
16. I. Aramori and S. Nakanishi, *Neuron* **8**, 757 (1992).
17. P. M. Vassilev, J. Mitchel, M. Vassilev, M. Kanazirska, E. M. Brown, *Biophys. J.* **72**, 2103 (1997).
18. The cAMP level of CHO cells expressing mGluR 2 or 3 were measured as follows. Cells were cultured in GlutaMAX-free medium for 4 hours, then rinsed by and incubated in the measurement solution (140 mM NaCl, 4 mM KOH, 10 mM Hepes, 0.3 mM $MgCl_2$, 1 mM isobutyl-methylxanthine) at 37°C for 20 min. Cells were then incubated in the measurement solution with 10 μM forskolin and a ligand (glutamate or Ca^{2+}) at 37°C for 10 min. Cells were lysed by 5% trichloroacetic acid, and the cAMP levels were measured by the cAMP EIA system (Amersham) following the manufacture's protocol. In the experiment of mGluR1α-expressing cells, forskolin was not added.
19. Single-letter abbreviations for the amino acid residues are as follows: A, Ala; C, Cys; D, Asp; E, Glu; F, Phe; G, Gly; H, His; I, Ile; K, Lys; L, Leu; M, Met; N, Asn; P, Pro; Q, Gln; R, Arg; S, Ser; T, Thr; V, Val; W, Trp; and Y, Tyr.

20. We thank S. Nakanishi for providing us with rat mGluRs 1α through 7 cDNA clones and CHO cell line expressing mGluR2; N. Sekiyama for teaching us techniques of cell culture and the cAMP measurement; M. Lazdunski and J. Miyazaki for GIRK2 cDNA and $pCXN_2$ vector, respectively; R. Murrell-Lagnado for comments on the manuscript; and K. Kubokawa, H. Okado, and K. Takahashi for discussion. Supported by research grants from the ministry of Education, Science, Sports and Culture of Japan for Exploratory Research to Y.K. and for scientific research on the priority area of "Channel-Transporter Correlation" to Y.K. Y.K. is also supported by Core of Research for Evolutional Science and Technology of the Japan Science and Technology Corporation.

18 November 1997; accepted 15 January 1998

Hyperinnervation of Neuromuscular Junctions Caused by GDNF Overexpression in Muscle

Quyen T. Nguyen,* Alexander Sh. Parsadanian,* William D. Snider, Jeff W. Lichtman†

Overexpression of glial cell line–derived neurotrophic factor (GDNF) by muscle greatly increased the number of motor axons innervating neuromuscular junctions in neonatal mice. The extent of hyperinnervation correlated with the amount of GDNF expressed in four transgenic lines. Overexpression of GDNF by glia and overexpression of neurotrophin-3 and neurotrophin-4 in muscle did not cause hyperinnervation. Thus, increased amounts of GDNF in postsynaptic target cells can regulate the number of innervating axons.

Experimental application of growth factors can alter the density and distribution of axon branches (*1*); hence, growth factor release may be one means by which target cells regulate the number of synaptic connections they receive (*2*, *3*). We sought to test this idea in a system where the complement of axon branches innervating a target cell could be visualized and functionally assessed. We generated mice in which muscle fibers synthesized excess amounts of a specific neurotrophic factor, GDNF, and studied innervation at the neuromuscular junction (NMJ). GDNF was chosen because it is perhaps the most potent survival factor for motor neurons, both in vitro and in vivo (*4*–*6*). In addition, GDNF is synthesized by muscle and Schwann cells (*4*, *7*, *8*) and is internalized and specifically transported retrogradely by motor neurons through a receptor-mediated process (*6*).

To examine the effect of increased target-derived GDNF on NMJ development, we generated several lines of *Myo-GDNF* mice (*9*) that overexpress GDNF under a muscle-specific (myogenin) promoter (*10*, *11*) (Fig. 1A). The myogenin promoter was chosen because it drives transgene expression in muscle beginning in embryogenesis, about the time axons first approach muscle fibers, and continues expression into postnatal life (*10*).

Q. T. Nguyen and J. W. Lichtman, Department of Anatomy and Neurobiology, Washington University School of Medicine, St. Louis, MO 63110, USA.
A. Sh. Parsadanian and W. D. Snider, Department of Neurology, Washington University School of Medicine, St. Louis, MO 63110, USA.

*These authors contributed equally to this report.
†To whom correspondence should be addressed. E-mail: jeff@thalamus.wustl.edu